Effect of a mixed-in crystallization inhibitor on the properties of hydraulic mortars

Kamat, A.A.; Lubelli, B.; Schlangen, E.

DOI
10.3934/matersci.2022038

Publication date
2022

Document Version
Final published version

Published in
AIMS Materials Science

AIMS Materials Science, 9(4): 628–641.
DOI: 10.3934/matersci.2022038
Received: 15 June 2022
Revised: 26 July 2022
Accepted: 9 August 2022
Published: 16 August 2022

http://www.aimspress.com/journal/Materials

Research article

Effect of a mixed-in crystallization inhibitor on the properties of hydraulic mortars

Ameya Kamat[1,2]*, Barbara Lubelli[1] and Erik Schlangen[2]

[1] Heritage and Architecture, Architecture and Built Environment, Delft University of Technology, The Netherlands
[2] Materials and Environment, Civil Engineering and Geosciences, Delft University of Technology, The Netherlands

* **Correspondence:** Email: a.a.kamat@tudelft.nl; Tel: +31(0)15 2781116.

Abstract: Porous building materials are often subjected to damage due to salt crystallization. In recent years, the addition of crystallization inhibitors in lime-based mortar, has shown promising results in improving durability of this material against salt decay. Lime-based mortars have low mechanical properties and slow setting. They are often replaced with hydraulic binders to overcome these limitations. However, the effect of crystallization inhibitors in mortars with hydraulic binders is still unknown. Incorporation of crystallization inhibitors in hydraulic mortars would widen the application field of this new technology. In this research, the possibility to develop hydraulic mortars with mixed-in sodium ferrocyanide, an inhibitor of sodium chloride crystallization, is explored. As an essential first step, the influence of this inhibitor addition on the properties of hydraulic mortars is investigated. Two common types of hydraulic binders, natural hydraulic lime (NHL) and ordinary Portland cement (CEM I), were studied; the inhibitor was added in different amounts (0%, 0.1% and 1% by binder weight) during mortar (and binder paste) preparation. Relevant mortar and binder paste properties, in fresh (hydration, workability, setting time) and hardened (mechanical strength, elastic modulus, pore size distribution, water absorption) state, were assessed using several complementary methods and techniques. The results indicate that the addition of ferrocyanide does not alter the studied properties of both NHL and CEMI-based mortar and binder pastes. These results are promising for the further development of hydraulic mortars with an improved durability with respect to salt decay.

Keywords: salt damage; crystallization inhibitor; hydraulic mortar; durability; sodium ferrocyanide

1. Introduction

Salt crystallization in porous building materials (e.g., bricks and mortar) induces stresses [1] and is a recurrent/main cause of damage in buildings. Salt damage is particularly evident in plasters and renders making them vulnerable to salt decay, owing to various reasons. Due to their proximity to the outer, evaporative surface of the walls, plasters and renders are the location where salts tend to accumulate and undergo dissolution and crystallization cycles in response to changing environment (RH and temperature changes, rain etc.).

Plaster and renders show therefore often a limited durability in the presence of moisture and salts. Different solutions have been proposed to improve the service life of these materials, such as the use of water repellent additives mixed in the mass (the so-called salt accumulating plasters) [2]). However, the durability of such solutions is limited and their compatibility with existing (historic) buildings is low, especially in the presence of high moisture content in the underlying masonry. Alternative solutions have been therefore sought to improve the durability of plaster and render mortars against salt decay. In the past years, the use of crystallization inhibitors has been considered as a potentially durable solution against salt decay.

Crystallization inhibitors are molecules that alter the process of crystallization by delaying nucleation and/or by modifying the crystal habit [3]. Alkali ferrocyanides (FeCN) have been shown to be effective in inhibiting NaCl growth and are commonly used as anti-caking agents [4]. In studies performed on bulk solutions, the presence of FeCN has shown to alter sodium chloride crystal morphology from a cubic habit to a dendritic pattern having a higher surface area [5]; this habit modification has shown to increase the rate of evaporation [6]. In early studies, the inhibitor was introduced in the building materials with salt solutions through capillary absorption. Researchers observed a larger amount of efflorescence in materials contaminated with an aqueous solution of NaCl and FeCN with respect to materials contaminated with NaCl solution, suggesting increased salt transport outside the porous substrate [6–8]. This was been attributed to both the inhibition of crystal nucleation, leading to a higher advection of salt ions to the surface, and to the faster evaporation rate, induced by the large evaporation surface of the branched crystals [9]. As per Granneman et al. [3], FeCN in porous materials leads to an increase in NaCl nucleation density due to high supersaturation and consequently smaller crystals. This is also thought to reduce pore clogging and lower crystallization pressure in the pores.

A study revealed that FeCN was effective only if added prior to crystallization (when Na and Cl are present as ions) whereas, its effect on modifying salt crystals and/or favoring their dissolution was not evident [6,10]. Thus, for the inhibitor to be effective, it must be present in the building materials before salt crystallization takes place. In mortars, a way to obtain these conditions is to add the inhibitor during mortar preparation. This approach was tested for the first time with promising results in air-hardening, (hydrated) lime-based mortars, to which sodium FeCN was added [11]. The lime mortar with mixed-in inhibitor showed an increased resistance to salt decay, in comparison to mortar without the inhibitor under an accelerated salt weathering test [12,13], while showing a negligible effect on relevant physical/chemical properties of mortar [14].

Hydrated lime-based mortars are often used in restoration works owing to good compatibility with historic materials. However, in renovation works and new constructions, hydrated lime mortars have been replaced with hydraulic mortars, on account of higher mechanical strength and faster setting. Even in the field of restoration, natural hydraulic lime as well as blended cement-lime mortars are seen to be potential alternatives to overcome limitations of traditional lime mortars [15–19]. Nonetheless, hydraulic mortars remain vulnerable to salt decay and the use of crystallization inhibitors can be

beneficial in improving their durability in those cases where moisture and salts are present.

Until now, the potential for the use of crystallization inhibitors in hydraulic mortars has not been yet explored, which is limiting its application. The different mechanism of strength gain and setting between hydrated lime mortars and hydraulic mortars, may invalidate the positive results observed in the case of hydrated lime mortars with FeCN. In fact, whereas in hydrated lime mortars, carbonation is solely responsible for microstructure development, in hydraulic mortars hydration (i.e., exothermic reaction between water and the binder) plays a primary role. In order to extend the concept of mixed in crystallization inhibitors to hydraulic mortars, therefore, a first essential step towards the developments of hydraulic mortar with mixed-in inhibitor, consists in assessing if any interaction occurs between the inhibitor and the hydraulic binders (e.g., NHL or Portland Cement) that could negatively affect the mortar properties and/or performance.

This paper investigates the effect of sodium ferrocyanide on the properties of hydraulic mortars prepared with NHL and CEMI binders, by means of tests and experiments carried out in laboratory.

2. Materials and methods

2.1. Building materials

Two types of hydraulic binders were tested, natural hydraulic lime (NHL) with a strength class of 3.5 and ordinary Portland cement (CEM I) with a strength class of 42.5. Standard river sand, as per EN 196-1 with a particle size distribution of 0.08–2 mm was used to prepare mortar specimens [20]. Sodium ferrocyanide decahydrate ($Na_4Fe(CN)_6{\cdot}10H_2O$) (Sigma Aldrich) was used as the crystallization inhibitor.

2.2. Specimen preparation and storage conditions

Two types of specimens were prepared for performing various tests, namely, binder-paste specimens and mortar specimens.

2.2.1. Binder paste specimens

Control specimens (without inhibitor) were prepared by mixing binder and demineralised water to form a paste. The water-binder ratio (w/b) was maintained at 1 and 0.5 by weight for NHL and CEM I respectively.

To prepare specimens with mixed in inhibitor, sodium ferrocyanide decahydrate (FeCN) was first dissolved in demineralized water and subsequently added to the binder to form a paste. Specimens with different inhibitor concentrations were prepared: 0.01%, 0.1% and 1% (weight of the inhibitor is expressed as a percentage of the binder weight). The concentrations were selected based on previous research [3,6]. Paste specimens were immediately tested (heat of hydration and setting time) in their fresh state.

2.2.2. Mortar specimens

Mortar specimens were prepared according to the European standards, EN 459-2 [21] for NHL and EN 196-1 [20] for CEM I. Binder and sand were weighed in a 1:3 ratio. This ratio was chosen as per the standards to test the binder strength and was used for all the other tests to make meaningful

comparisons. FeCN specimens were prepared with concentrations of 0.1% and 1% by weight of the binder. FeCN was first dissolved in the water used for the preparation of the mortar. The water-binder ratio (w/b) was fixed at 0.5 for CEM I and 0.6 for NHL. Additionally, control specimens (without inhibitor) were prepared as a reference.

Mortar specimens were cast as prisms as well as slabs. Prisms were used for assessing the mechanical properties and the slabs were used to study transport related properties. Prisms were cast in polystyrene molds with dimension 160 × 40 × 40 mm and were compacted using a vibrating table as per EN 196-1 [20]. Mortar slabs were cast on a fired-clay brick and compacted by hand to obtain field comparable mortar which is more representative for studying moisture transport [22,23]. A paper towel was placed on top of the brick before casting the mortar, to facilitate demolding of the mortar slabs. The slabs had a size of 200 × 100 mm with a thickness of 20 mm.

After casting, all mortar specimens were covered in plastic and stored at lab conditions for the first 24 h. CEM I specimens were demolded/ detached from the brick substrate after 24 h and transferred to the curing room. NHL specimens were transferred to the curing room after 24 h with the molds and demolded/detached on day 5, in order to prevent damage during demolding on account of slower hydration. The conditions in the curing room were maintained at 20 ℃ / > 95% RH. Specimens were stored in the curing room until tested, to minimize carbonation.

3. Test methods

Various tests were performed on the paste and mortar specimens to assess the effect of the inhibitor on early age (fresh) properties and hardened properties of the mortars. A summary of the test methods, specimen number and size are presented in Table 1.

Table 1. Overview of test methods and specimens.

Measured properties	Test method	Specimen type	Binder type	Inhibitor (%)[1]	Replicates	Size/ weight (mm/g)
heat of hydration	Isothermal Calorimetry	Binder paste	NHL3.5 CEM I	0, 0.01, 0.1, 1	2	~7.5
setting time	Vicat penetration	Binder paste	NHL3.5 CEM I	0 1	2	-
workability	Flow table test	Fresh mortar	NHL3.5 CEM I	0, 0.1, 1	2	-
compressive /flexural strength	Compression/ 3-point bending	Mortar prisms	NHL3.5 CEM I	0, 0.1, 1	3	160 × 40 × 40
e-modulus	Compression test	Mortar prisms	NHL3.5 CEM I	0, 0.1, 1	3	160 × 40 × 40
open porosity/pore size distribution	MIP/N2	Mortar slabs	NHL3.5 CEM I	0, 0.1, 1	2	~4/1
moisture transport	Capillary absorption/drying	Mortar slabs	NHL3.5 CEM I	0, 0.1, 1	4	50 × 20 × 20

[1] Percentage of binder weight

3.1. Characterization of early age/fresh properties

3.1.1. Measurement of heat of hydration

The primary mechanism for the development of microstructure in hydraulic mortar takes place through hydration (reaction between binder and water). Since, the reaction is exothermic, monitoring the heat released during hydration provides indirect information on the microstructure development and the reaction products. The possible effects of binder-inhibitor interaction on early age reaction products can be thus captured.

The heat flow and the cumulative heat of hydration was measured on fresh binder paste specimens using an 8 channel thermometric isothermal calorimeter (TAM-Air). The test procedure is based on EN-196-11 [24]. Paste was prepared in the glass ampoule directly and placed in the calorimeter immediately. Quartz specimens with a known specific heat were used as a reference to eliminate background noise. The temperature of the calorimeter was set to 20 ± 0.2 ℃ and the heat evolution was monitored continuously for 168 h (7 d).

3.1.2. Setting time

Setting time is defined as the time required for the binder to completely lose its plasticity and attain a certain resistance to external pressure. The setting time of binder paste specimens, with and without the addition of the inhibitor, was measured using an automated Vicat Penetration test. The test was carried out according to EN 196-3 [25]. The depth of needle penetration was recorded automatically at fixed time intervals until the paste was completely set. The penetration curve was obtained as a function of time.

3.1.3. Workability

Workability refers to the measurement of consistency and in turn the ease of compaction/application during construction. A good workability is necessary for easy application of a mortar in practice. The workability was measured using a flow table test as per EN-1015-3 [26]. Freshly mixed mortar was placed on a standard flow table in a cone in two steps. The table was jolted 15 times at a rate of 1 jolt/s. Two diametric readings of the flow were recorded and the mean value reported.

3.2. Characterization of Hardened properties

3.2.1. Measurement of compressive strength, flexural strength and elastic modulus

Compressive and flexural strength are indicative of load bearing capacities and to an extent durability of mortars. Whereas, elastic modulus provides information about stiffness of mortar and its ability to accommodate movements. Compression and flexural strength were measured on mortar prisms following EN 1015-11 norm [27]. The loading rate was maintained at 2.4 kN/s and 0.1 kN/s for compression and flexural test for CEM I specimens. In case of NHL specimens, the loading rate was reduced to 0.1 kN/s and 5 N/s for compression and flexural strength respectively. The test was performed at 28 d and at 90 d, to capture the short term and the long term mechanical effects.

Elastic modulus was measured on mortar prisms using an Instron universal testing machine. 4

Linear Variable Differential Transformer (LVDT) were glued to the specimen on the 4 sides to record the deformation (Figure 1a). The specimens were subjected to three compressive loading and unloading cycles (Figure 1b). The maximum force that the specimens were subjected to was limited to 9.5 kN (5.9 MPa) for CEM I and 3 kN (1.87MPa) for NHL, in order to stay within the elastic limits. The elastic modulus was calculated as the ratio of the applied stress to the measured strain. The test was carried out on 28th day after casting.

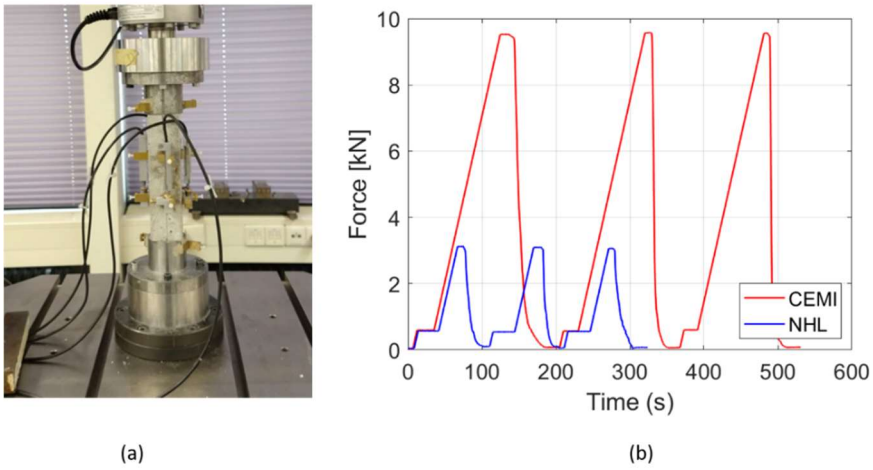

Figure 1. (a) Experimental setup for measuring Young's modulus. Displacement measured using LVDT (b) Applied loading-unloading cycles for E-modulus measurements.

3.2.2. Porosity and pore size distribution

Mercury intrusion porosity (MIP) was used to measure open porosity and the pore size distribution of the mortar specimens. The test was performed in Autopore IV series machine from Micromeritics. Solid samples were collected from the middle of the mortar slabs after 28 d of curing and were dried in a freeze drier to a constant weight. This was done to remove the moisture as well as prevent further hydration. Approximately, 4 g of sample was used on 2 replicates. The samples were subjected to a maximum intrusion pressure of 210 MPa and the contact angle between the mercury and the samples was assumed to be 141°. These conditions facilitated pore throat measurements between 400 μm and 0.01 μm.

In addition to MIP, N_2 adsorption method was used to obtain the pore size distribution of pores smaller than 0.01 μm. Micromeritics Gemini VII machine was used for the test. The test was performed on ~1 g of freeze dried specimens. The size of the fragments that were tested were between 2–4 mm.

3.2.3. Measurement of water absorption and drying rate

The moisture transport properties of the mortars with the inhibitor and without the inhibitor were assessed through capillary absorption followed by drying. EN 1925 [28] was used as a guideline for capillary absorption. 50 × 50 × 20 mm specimens were cut using a saw from the mortar slabs after 28 days of curing. 4 specimens from 4 different slabs were used as replicates, in order to keep the sampling representative. The specimens were first dried in an oven at 40 °C until a constant weight was obtained. The lateral sides of the specimens were sealed using paraffin film to have a uni-directional moisture

flow. The base of the specimens was in immersed in water to facilitate capillary absorption. The immersion level of the water was kept constant. Samples were weighed at prescribed time intervals with a precision of 0.01 g. For NHL, the time intervals as per the high absorbing substrate guidelines were used whereas, for CEM I, the time intervals as per the low absorbing substrate guidelines were used [28]. Two stages of water absorption with distinct slopes were recorded. The water absorption coefficient (WAC) calculated from Eq 1.

$$WAC = \frac{W_i - W_0}{A.(\sqrt{t_i} - \sqrt{t_0})} \quad (1)$$

Where, W_0 is the dry weight of the specimen at time t_0. W_i is the weight of the specimen at time t_i which is the time at which transition between two absorption stages occur. A is the surface of the specimen in contact with water.

Following capillary absorption, the specimens were dried in the oven at 40 °C. The weight of the specimens was recorded regularly to obtain a drying curve. The measurements were performed until the specimens reached a constant weight.

4. Results and discussion

4.1. Effect of ferrocyanides on early age/ fresh properties

The results obtained from the heat of hydration measured using isothermal calorimeter are presented in Figure 2. The results are normalized to the weight of the specimen for comparative purposes. The hydration behavior in CEM I is different to that of NHL due to different proportions of hydraulic phases (e.g., Alite (C_3S) and Belite (C_2S) phases) [29]. A higher heat was generated in CEM I than in NHL: this is due to the presence of higher amount of C_3S in CEM I; differently in NHL specimens C_2S is the dominant hydraulic phase. However, irrespective of the binder and their hydraulic components, the difference in the cumulative heat evolution between specimens with and without inhibitor negligible. The presence of FeCN ions in the pore solution do not seem to interact or form products with different hydraulic phases in CEMI or NHL.

The results of the Vicat penetration test (Figure 3) show that the penetration curve obtained in time is unaffected by the addition of inhibitor for both CEM I and NHL. The intitial and final setting times for specimens with the inhibitor and without the inhibitor are comparable to each other.

The results of the workability measurements (Tables 2,3), show a minor increase in flow for CEM I specimens in which the inhibitor was added. On the other hand, a slight decrease in flow for NHL specimens. Considering the variation observed in the data, a correlation between addition of the inhibitor and the flow test cannot be clearly established; in any case the impact of the inhibitor on the workability of the mortar is minor.

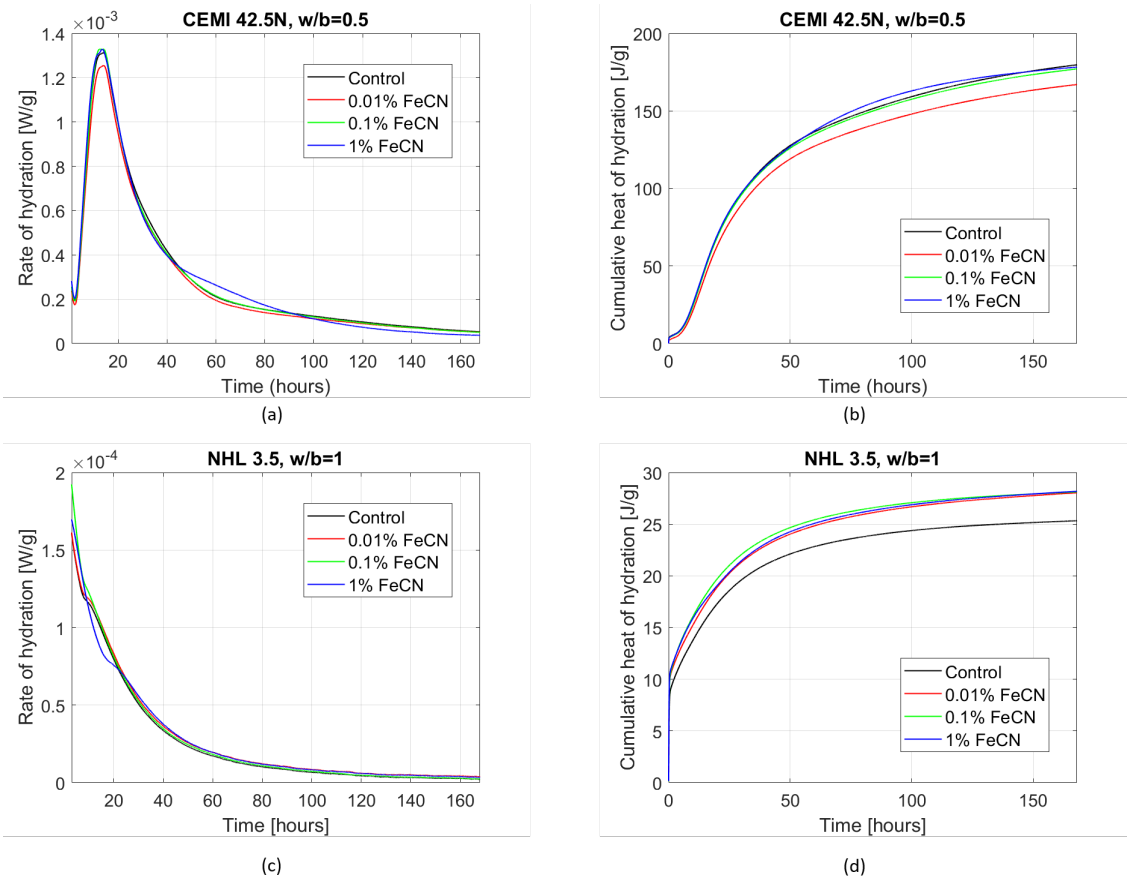

Figure 2. (a) Rate of hydration for CEMI (b) Cumulative heat of hydration for CEM I (c) Rate of hydration for NHL (d) Cumulative heat of hydration for NHL.

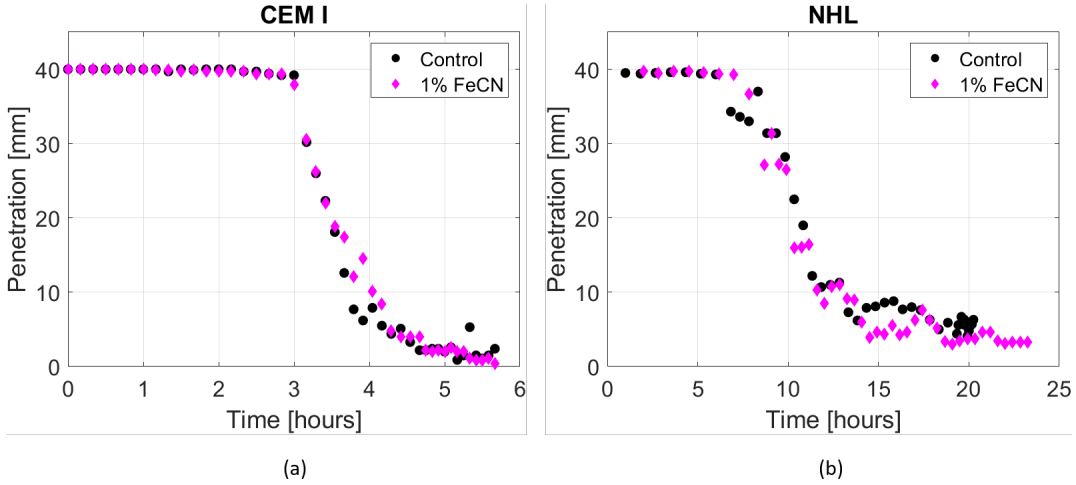

Figure 3. Vicat penetration test for (a) CEM I paste (b) NHL paste.

4.2. Effect of ferrocyanides on hardened properties of mortar

The mechanical properties measured on mortar prisms are reported in Table 2 for CEM I and Table 3 for NHL. The results obtained for specimens with and without the inhibitor, at both 28 d

and 90 d, show minor differences. The compressive (f_c) and flexural strength (f_b) observed at 90 d is higher than that at 28 d, as expected due to continued hydration.

In case of NHL specimens, the 28th day elastic modulus shows some scatter, but the values are not necessarily in the proportion of the added FeCN. The large scatter observed in NHL mortars is attributed to possible micro-cracking during cyclic loading. The applied maximum load of 1.87 MPa (50% of compressive strength) in combination with NHL's low mechanical strength probably induced inelastic behavior in some specimens.

Table 2. Comparison of CEMI mortar properties with different inhibitor content.

Measured property	Control ($\mu^1 \pm \sigma^2$)	0.1% FeCN ($\mu \pm \sigma$)	1% FeCN ($\mu \pm \sigma$)
Flow [mm]	151.7 ± 5.7	164 ± 4.6	165.7 ± 6.3
$f_{c\ 28\ d}$ [MPa]	38.87 ± 1.69	37.29 ± 1.3	36.83 ± 2.8
$f_{c\ 90d}$ [MPa]	41.02 ± 4.08	39.61 ± 2.88	37.82 ± 2.55
$f_{b\ 28d}$ [MPa]	7.12 ± 0.8	8.14 ± 0.61	8.23 ± 0.29
$f_{b\ 90d}$ [MPa]	8.13 ± 0.75	8.06 ± 0.07	7.56 ± 0.4
E-modulus $_{28\ d}$ [MPa]	35529 ± 1511	37105 ± 2514	35900 ± 2590
WAC [$g/m^2s^{0.5}$]	13.16	13.95	14.53
Open Porosity [%]	11.75	10.98	11.41

1 mean and 2 standard deviation.

Table 3. Comparison of NHL mortar properties with different inhibitor content.

Measured property	Control ($\mu \pm \sigma$)	0.1% FeCN ($\mu \pm \sigma$)	1% FeCN ($\mu \pm \sigma$)
Flow [mm]	143.2 ± 1.8	139 ± 3.7	136.5 ± 2.1
$f_{c\ 28\ d}$ [MPa]	3.22 ± 0.24	3.52 ± 0.06	3.75 ± 0.09
$f_{c\ 90\ d}$ [MPa]	5.64 ± 0.87	5.88 ± 0.2	6.28 ± 0.48
$f_{b\ 28\ d}$ [MPa]	1.30 ± 0.02	1.44 ± 0.13	1.44 ± 0.04
$f_{b\ 90\ d}$ [MPa]	2.23 ± 0.87	2.62 ± 0.07	2.65 ± 0.13
E-modulus $_{28\ d}$ [MPa]	3441 ± 1025	4324 ± 879	3217 ± 811
WAC [$g/m^2s^{0.5}$]	137.11	123.46	131.97
Open Porosity [%]	23.44	23.51	23.54

1 Mean and 2 standard deviation.

The pore size distribution for CEM I and NHL mortars, as measured by MIP (pore diameter between 100 μm and 0.01 μm) and N_2 adsorption (pore diameter less than 0.01 μm) is presented in Figure 4. The average mean pore diameter of around 0.05 μm and 0.15 um was obtained for CEM I and NHL respectively, irrespective of the amount of inhibitor. The cumulative intrusion obtained for mortar specimens with and without FeCN is almost identical. The open porosity, as measured by MIP for CEM I (~11.3%) and NHL (~23%), does not change significantly with the addition of the inhibitor. The pore size distribution for pores smaller than 0.01 μm is also unaffected (Figures 4b,d). Based on these results, it can be concluded that FeCN does not alter the pore structure in the studied hydraulic mortars.

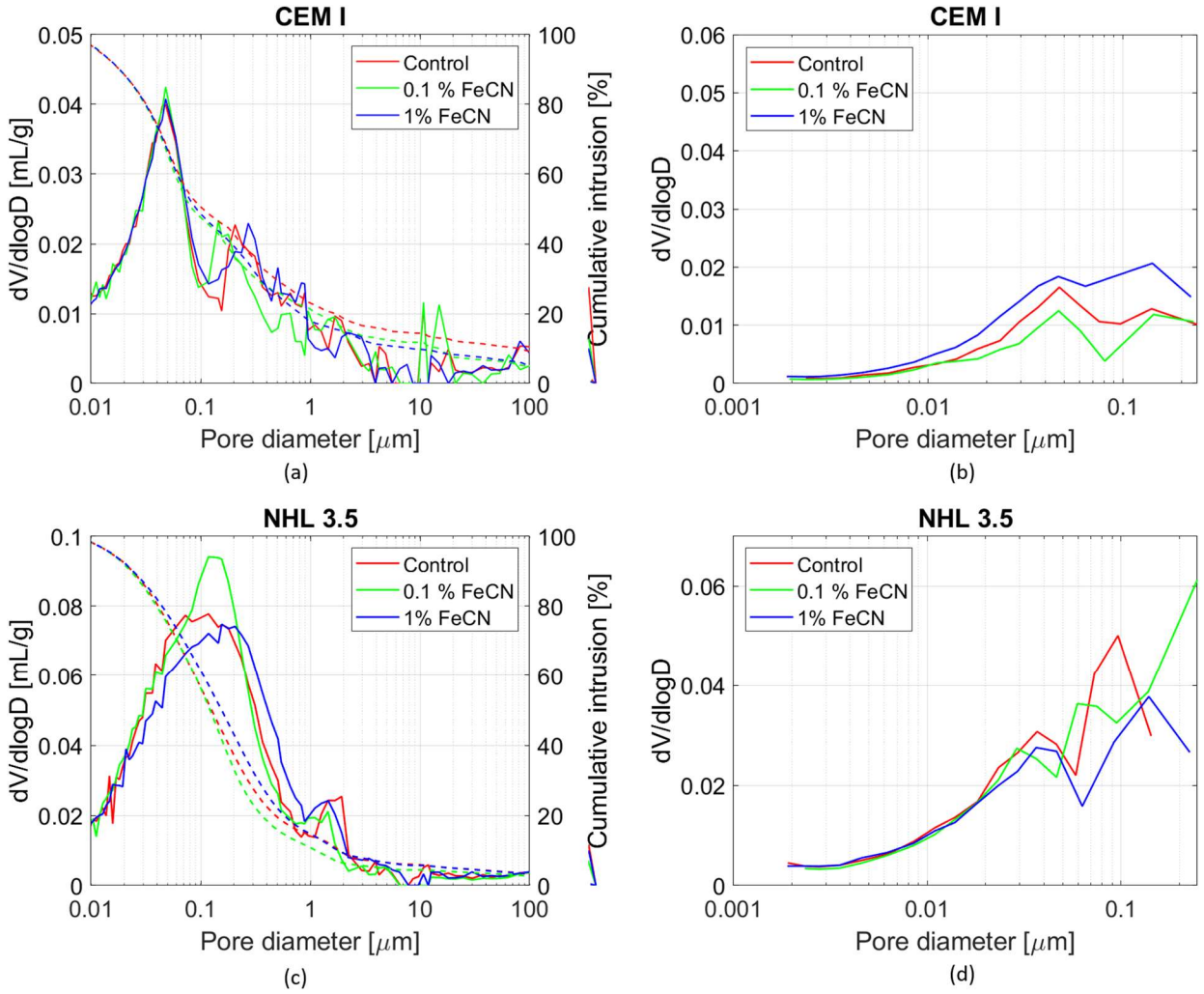

Figure 4. Pore size distribution measurements (a) MIP for CEM I (b) N_2 adsorption for CEMI (c) MIP for NHL (d) N_2 adsorption for NHL.

The capillary water absorption curves for CEMI and NHL mortar specimens with and without inhibitor is shown in Figure 5. The water absorption is normalized to the dry weight of the specimens to take into account the thickness variation across specimens resulting from hand compaction. The two stages of absorption can be distinctly seen for both CEM I and NHL. Linear regression was performed on two absorption stages and the intersection point was used to calculate the water absorption coefficient (WAC) as per Eq 1. The WAC values for different inhibitor contents, as shown in Table 2 (CEM I) and Table 3 (NHL), are comparable to their respective control specimens. Moreover, the normalized water absorption curves (Figure 5) in both the absorption stages show negligible differences between specimens with and without inhibitor.

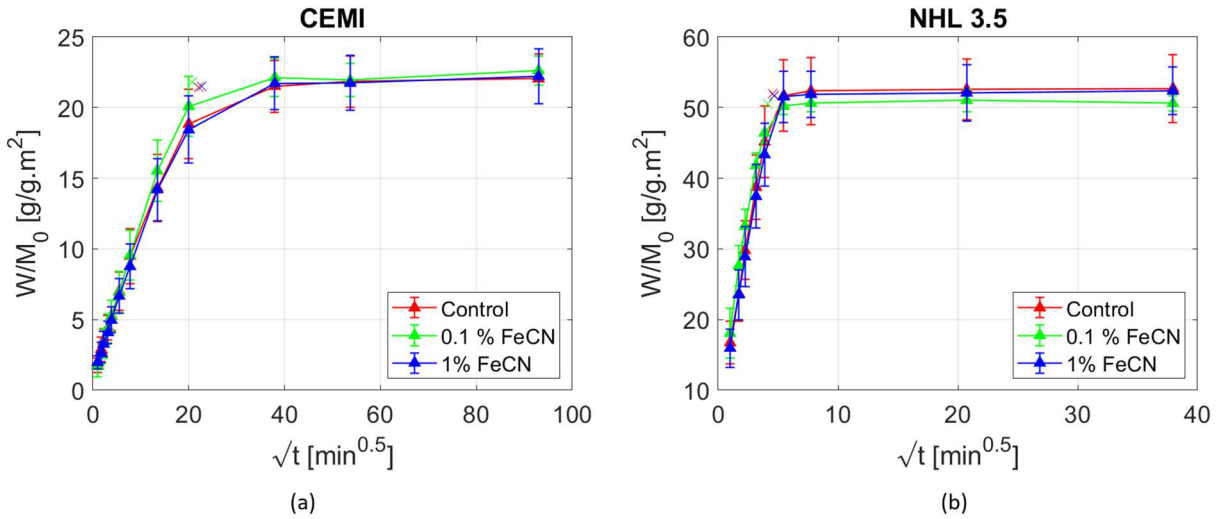

Figure 5. Moisture absorption through capillarity for different FeCN concentrations (a) CEMI (b) NHL.

The drying behavior of CEM I and NHL is shown in Figure 6. In case of CEM I (Figure 6a), the specimens with FeCN dry slightly slower than the control specimens. However, considered the high scatter observed in the drying curves of the control specimens, the effect of inhibitor on the drying can be judged to be minor. In the case of NHL specimens, the drying curves for specimens with and without FeCN addition are very similar. Based on these results, and taking into account the outcome of the pore size distribution, it can be concluded that the moisture transport properties are not significantly affected by the addition of FeCN.

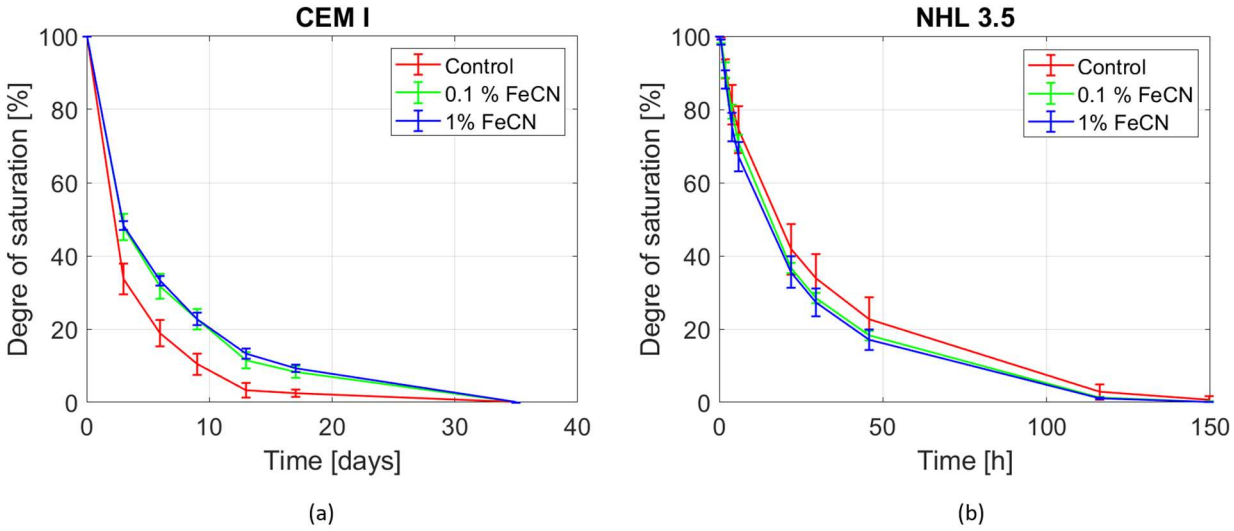

Figure 6. Drying behavior of mortar specimens with different FeCN concentration (a) CEMI (b) NHL.

5. Conclusion

In this paper, the interaction between sodium ferrocyanide, a well-known inhibitor of NaCl crystallization, and two types of hydraulic binders (NHL and OPC) was studied. Various properties of the binders in fresh paste and of the fresh and hardened mortars were assessed on specimens with different inhibitor concentrations (0%, 0.01%, 0.1% and 1%). The results of all the measurements agree with each other and clearly show that the addition of inhibitor, up to 1%, of the binder weight does not affect the mechanical and moisture transport properties in the studied hydraulic mortars. The hydration of binder paste as well as the setting time is unaffected by the addition of the inhibitor. Therefore, it can be inferred from the results that sodium ferrocyanide remains inert and does not participate in development of the microstructure of the studied mortars. Sodium ferrocyanide thus proves to be a suitable crystallization inhibitor that can be added during the mixing stage.

These results constitute a first step in the development of hydraulic mortars with crystallization inhibitors, opening new possibilities for the wider use of this inhibitor in different applications, from building renovation to new construction.

In future work, the durability of the hydraulic mortars with mixed-in FeCN with respect to salt decay will be assessed, both in laboratory and in situ.

Acknowledgments

The research is supported by the funding of NWO under the umbrella of the project 'Mortars with mixed-in inhibitors for mitigating salt damage-MORISAL' (Project No. 17636). The authors would like to thank Mr. Maiko van Leeuwen and Mr. Arjan van Thijssen for their help with technical assistance in laboratory tests.

Conflict of interest

The Authors declare that there is no conflict of interest.

References

1. Scherer GW (2004) Stress from crystallization of salt. *Cem Concr Res* 34: 1613–1624. https://doi.org/10.1016/j.cemconres.2003.12.034
2. Hees RPJ Van, Naldini S, Delgado J (2008) Plasters and renders for salt laden substrates. *Constr Build Mater* 23: 1714–1718. https://doi.org/10.1016/j.conbuildmat.2008.09.009.
3. Granneman SJC, Lubelli B, van Hees RPJ (2019) Mitigating salt damage in building materials by the use of crystallization modifiers–a review and outlook. *J Cult Herit* 40: 183–194. https://doi.org/10.1016/j.culher.2019.05.004.
4. Bode AAC, Vonk V, Van Den Bruele FJ, et al. (2012) Anticaking activity of ferrocyanide on sodium chloride explained by charge mismatch. *Cryst Growth Des* 12: 1919–1924. https://doi.org/10.1021/cg201661y.
5. Townsend ER, Van Enckevort WJP, Meijer JAM, et al. (2017) Additive Enhanced Creeping of Sodium Chloride Crystals. *Cryst Growth Des* 17: 3107–3115. https://doi.org/10.1021/acs.cgd.7b00023.

6. Rodriguez-Navarro C, Linares-Fernandez L, Doehne E, et al. (2002) Effects of ferrocyanide ions on NaCl crystallization in porous stone. *J Cryst Growth* 243: 503–516. https://doi.org/10.1016/S0022-0248(02)01499-9.
7. Lubelli B, van Hees RPJ (2007) Effectiveness of crystallization inhibitors in preventing salt damage in building materials. *J Cult Herit* 8: 223–234. https://doi.org/10.1016/j.culher.2007.06.001.
8. Rivas T, Alvarez E, Mosquera MJ, et al. (2010) Crystallization modifiers applied in granite desalination: The role of the stone pore structure. *Constr Build Mater* 24: 766–776. https://doi.org/10.1016/j.conbuildmat.2009.10.031.
9. Gupta S, Terheiden K, Pel L, et al. (2012) Influence of ferrocyanide inhibitors on the transport and crystallization processes of sodium chloride in porous building materials. *Cryst Growth Des* 12: 3888–3898. https://doi.org/10.1021/cg3002288.
10. Selwitz C, Doehne E (2002) The evaluation of crystallization modifiers for controlling salt damage to limestone. *J Cult Herit* 3: 205–216. https://doi.org/10.1016/S1296-2074(02)01182-2.
11. Lubelli B, Nijland TG, Van Hees RPJ, et al. (2010) Effect of mixed in crystallization inhibitor on resistance of lime-cement mortar against NaCl crystallization. *Constr Build Mater* 24: 2466–2472. https://doi.org/10.1016/j.conbuildmat.2010.06.010.
12. Granneman SJC, Lubelli B, van Hees RPJ (2019) Effect of mixed in crystallization modifiers on the resistance of lime mortar against NaCl and Na2SO4 crystallization. *Constr Build Mater* 194: 62–70. https://doi.org/10.1016/j.conbuildmat.2018.11.006.
13. Feijoo J, Ergenç D, Fort R, et al. (2021) Addition of ferrocyanide-based compounds to repairing joint lime mortars as a protective method for porous building materials against sodium chloride damage. *Mater Struct* 54: 1–20. https://doi.org/10.1617/s11527-020-01596-4.
14. Granneman SJC, Lubelli B, Van Hees RPJ (2018) Characterization of lime mortar additivated with crystallization modifiers. *Int J Archit Herit* 12: 849–858. https://doi.org/10.1080/15583058.2017.1422570.
15. Maravelaki-Kalaitzaki P, Bakolas A, Karatasios I, et al. (2005) Hydraulic lime mortars for the restoration of historic masonry in Crete. *Cem Concr Res* 35: 1577–1586. https://doi.org/10.1016/j.cemconres.2004.09.001.
16. Silva BA, Ferreira Pinto AP, Gomes A (2015) Natural hydraulic lime versus cement for blended lime mortars for restoration works. *Constr Build Mater* 94: 346–360. https://doi.org/10.1016/j.conbuildmat.2015.06.058.
17. Silva BA, Ferreira Pinto AP, Gomes A (2014) Influence of natural hydraulic lime content on the properties of aerial lime-based mortars. *Constr Build Mater* 72: 208–218. https://doi.org/10.1016/j.conbuildmat.2014.09.010.
18. Mosquera MJ, Silva B, Prieto B, et al. (2006) Addition of cement to lime-based mortars: Effect on pore structure and vapor transport. *Cem Concr Res* 36: 1635–1642. https://doi.org/10.1016/j.cemconres.2004.10.041.
19. Arandigoyen M, Alvarez JI (2007) Pore structure and mechanical properties of cement-lime mortars. *Cem Concr Res* 37: 767–775. https://doi.org/10.1016/j.cemconres.2007.02.023.
20. European Committee for Standardization (2015) *Methods of testing cement–Part 1: Determination of strength*, Netherland: Committee for Standardization, NEN-EN 196-1.
21. European Committee for Standardization (2008) *Building lime–Part 2: Test methods*, Netherland: Committee for Standardization, NEN-EN 459-2.
22. Groot CJWP (1993) Effect of water on mortar-brick bond. *Heron* 40: 57–70.

23. Wijffels T, van Hees R (2000) The influence of the loss of water of the fresh mortar to the substrate on the hygric characteristics of so-called restoration plaster, *International Workshop on Urban Heritage and Building Maintenance VII*, 49–54.
24. European Committee for Standardization (2019) *Methods of testing cement–Part 11: Heat of hydration-Isothermal Conduction Calorimetry method*, Netherland: Committee for Standardization, NEN-EN 196-11.
25. European Committee for Standardization (2016) *Methods of testing cement–Part3: Determination of setting times and soundess*, Netherland: Committee for Standardization, NEN-EN 196-3.
26. European Committee for Standardization (1999) *Methods of test for mortar for masonry–Part 3: Determination of consistence of fresh mortar*, Netherland: Committee for Standardization, NEN-EN 1015-3
27. European Committee for Standardization (2019) *Methods of test for mortar for masnory–Part 11: Determination of flexural and conpressive strength of hardened mortar*, Netherland: Committee for Standardization, NEN-EN 1015-11.
28. European Committee for Standardization (1999) *Natural stone test methods–Determination of water absorption coefficient by capillarity*, Netherland: Committee for Standardization, NEN-EN-1925.
29. Lanas J, Bernal JLP, Bello MA, et al. (2004) Mechanical properties of natural hydraulic lime-based mortars. *Cem Concr Res* 34: 2191–2201. https://doi.org/10.1016/j.cemconres.2004.02.005.

AIMS Press